ACS OMEGA

Open Access

http://pubs.acs.org/journal/acsodf

Article

Microfluidic-Generated Injectable Bulking Agents with Biocompatible Surfaces and Their Mid-term Outcomes in a Rat Model with Anal Sphincter Injury

Joonbum Lee,[‖] Jung-Woo Choi,[‖] Sang-A Lee, Seokhyun Jang, Ji-Hun Seo,* and Kwang Dae Hong*

Cite This: *ACS Omega* 2024, 9, 43817−43825

Read Online

ACCESS | Metrics & More | Article Recommendations | Supporting Information

ABSTRACT: Bulking agents have gained attention as new, minimally invasive treatments for fecal incontinence. Various materials and surface treatment techniques have been extensively studied to ensure good biocompatibility and long-term stability. Despite significant improvements in biocompatibility, the nonuniform particle size of existing materials has led to other challenges, such as the induction of phagocytosis or reduction of injectability during in vivo tests. This study aimed to conduct a preclinical test of the midterm stability of bulking agents with newly formulated particles with uniform size. To this end, the particles were fabricated using microfluidics, resulting in a narrow size dispersity of less than 5% as the coefficient of variation, which is essentially distinct from conventional bulking agents. The microfluidic fabrication resulted in uniformly sized particles larger than the in vivo migratory limit of 80 μm and in a reduction in maximum injection pressure. Histological staining and microscopic observations confirmed proper positioning of the filler materials in vivo and a negligible immune response for up to 6 months, indicating successful midterm stability.

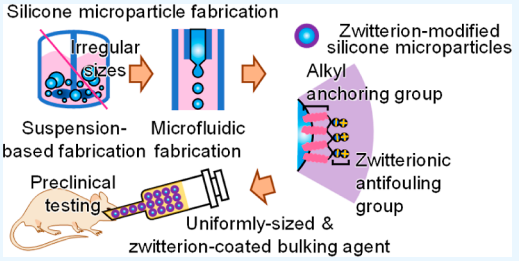

1. INTRODUCTION

Fecal incontinence (FI) is an involuntary stool leak that has multifactorial causes (e.g., diabetes mellitus, pregnancy, chronic diarrhea, anorectal surgery, and urinary incontinence). It can negatively impact the quality of life and lead to social isolation. There are various treatment options, and surgery is usually considered if there is no response to conservative treatments, such as antidiarrheal agents and biofeedback. Bulking agent injection around the anal sphincter is a minimally invasive procedure that can easily be performed in an outpatient clinic. The concept underlying this treatment is that bulking agents can augment the anal sphincter complex and act as passive barriers. This treatment showed significant midterm FI improvements and low adverse event rates.[1] Various materials have been developed for bulking agents, but none have yet had the properties of an ideal implant: biocompatibility, stability at the implantation site, no migration, and cost-effectiveness.[1−4]

The implantation of a biomaterial into the human body unavoidably induces a foreign-body reaction (FBR), comprising a series of inflammatory reactions followed by fibrosis.[5] Nonspecific protein adsorption onto the implant surface initiates a cascade of events that lead to the FBR.[3] Zwitterionic polymers are strongly hydrated and enable nonspecific protein resistance, which has shown promise as a coating material for medical catheters.[6−8] Thus, we developed a new bulking agent treated with a zwitterionic polymer on a polydimethylsiloxane (PDMS) surface to evade the initial immune reaction. Our earlier study showed that a filler surface treated with a zwitterionic polymer exhibited good biocompatibility in vitro, with 58% lower protein adsorption compared with that of a bulking agent without surface treatment.[9] However, this result was not reproduced in a rat FI model. We hypothesize that the observation period of the in vivo experiment was too short to improve the biocompatibility of the new bulking agent. Indeed, for medium- to long-term in vivo testing (e.g., 6 months or more), there is a need for remarkably improved stability. Nonetheless, existing filler materials, including those currently discussed in clinical trials and in our previous report, have a broad particle size distribution.[1,9] In such a broad particle size distribution, particles at both extremes of the size distribution can be problematic as injectable materials in vivo. Smaller particles can promote immune reactions, including phagocytosis, whereas larger particles can considerably reduce injectability during surgery. As a sequential result of reduced injectability, the wobble of the syringe needle during injection can cause injection site rupture or make it difficult for surgeons to guide properly the injection to the targeted site. The inaccurate filler location can further increase the loss of

Received: July 21, 2024
Revised: October 3, 2024
Accepted: October 8, 2024
Published: October 21, 2024

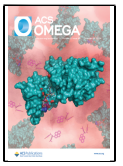

particles by body fluids, thus making it difficult to ensure long-term stability.[10−12] From a practical perspective, reoperation may be required if particles migrate or fragment, which could lead to further adverse outcomes.[13] Therefore, it is advantageous to generate a narrow distribution of particles that have the appropriate sizes.

In this study, we aimed to achieve a narrow size distribution of filler materials by adopting microfluidic fabrication (MF). MF is a technique used to fabricate microparticles with a highly uniform size distribution. Their possible drawback is the lack of productivity (low speed of production), which is also addressed when implementing diverse channel geometries, such as multichannels.[14] To confirm the resulting (improved) injectability, a methodology was newly developed to quantify injectability. Furthermore, by incorporating a zwitterionic polymer as a codispersant and surface modifier, as in previous studies, we investigated the 6 month, midterm biocompatibility of microparticles with uniform sizes prepared with enhanced biocompatibility (Figure 1).[9] To this end, the effects of MF on

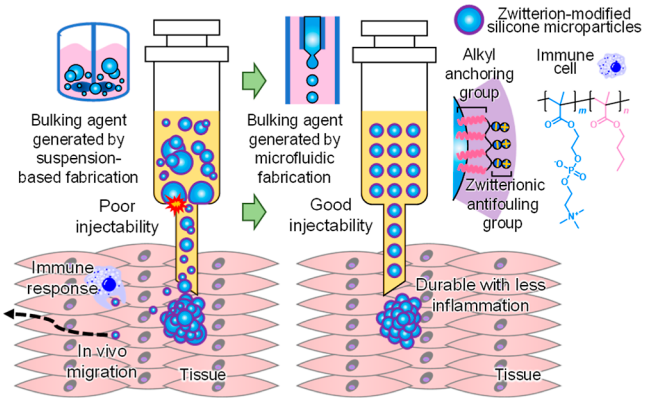

Figure 1. Schematic representation of the MF of the zwitterion-coated bulking agent and its midterm preclinical testing using a FI rat model.

microparticle size and injectability were first investigated, and the in vivo implantation of microparticles was rationalized by testing protein adsorption and cell cytotoxicity assays. The in vivo biocompatibility and therapeutic efficacy of the bulking material were investigated based on 6 month, midterm preclinical tests and results using a rat FI model.

2. METHODS

2.1. Materials. The compound 2-methacryloyloxyethyl phosphorylcholine (MPC) was purchased from KCI (Seoul, Republic of Korea), and *n*-butyl methacrylate (BPA) and 1,4-butanediol diglycidyl ether (BDDE) were purchased from Tokyo Chemical Industry (Tokyo, Japan). Anhydrous ethanol, diethyl ether, dichloromethane, and a sodium hydroxide solution (1 M) were purchased from Samchun Chemicals (Seoul, Republic of Korea). The 2,2′-azobis(isobutyronitrile) (AIBN) solution (0.2 M in toluene), poly(vinyl alcohol) (PVA), fluorescein isothiocyanate-labeled bovine serum albumin (FITC-BSA), and sodium nitrate were obtained from Sigma-Aldrich (Burlington, MA, USA). PDMS (Sylgard 184 silicone elastomer) was purchased from Dow (Midland, MI, USA), and hyaluronic acid (HA) sodium salt (91%, molecular weight ≥1 MDa, from *Streptococcus equi*) was purchased from Alfa Aesar (Ward Hill, MA, USA). Deionized water (DI) was obtained using a Milli-Q IQ 7000 ultrapure water system from Merck Millipore (Burlington, MA, USA). The SpectraPor regenerated cellulose dialysis membrane (with a molecular weight cutoff in the range of 12−14 kDa) was purchased from Repligen (Waltham, MA, USA). The NIH/3T3 mouse fibroblast cell line was obtained from the Korean Collection for Type Cultures. Phosphate-buffered saline (PBS) was purchased from Welgene (Gyeongsangbuk-do, Republic of Korea). Other bioreagents, including Dulbecco's PBS, trypsin-ethylenediaminetetraacetic acid solution (0.25%), Dulbecco's modified Eagle's medium, and newborn calf serum, were purchased from Invitrogen (Waltham, MA, USA). Water-soluble tetrazolium salt solution (Cell Counting Kit-8) for cell viability and proliferation assays was purchased from Dojindo (Kumamoto, Japan). The ^{1}H nuclear magnetic resonance (NMR) spectra of the synthesized copolymers were obtained using a Mercury NMR spectrometer (400 MHz) from Varian (Palo Alto, CA, USA). The molecular weight of the polymer was analyzed using a YL9100 gel permeation chromatography system from YL Instruments (Gyeonggi-do, Republic of Korea) with an Ultrahydrogel 1000 analytical column from Waters (Milford, MA, USA). Poly(ethylene oxide) standards and an aqueous sodium nitrate solution (0.2 M) were used as the mobile phases. NE-1000 syringe pumps were purchased from New Era Instruments (Farmingdale, NY, USA). The colorimetric measurements were performed using a Multiskan FC plate photometer from Thermo Fisher Scientific (Waltham, MA, USA). Microscopic images and routine cell cultures were obtained using an Eclipse Ts2-FL inverted microscope equipped with a DS-Fi3 color camera and NIS-Elements imaging software from Nikon (Tokyo, Japan). The compression forces were measured using a MultiTest-dV motorized force tester from Mecmesin (West Sussex, UK).

2.2. Synthesis of Zwitterionic Polymers. Synthesis of zwitterionic polymer was performed with slight modifications to the previous study.[15] Briefly, MPC (738.2 mg, 2.5 mmol) and BPA (355.5 mg, 2.5 mmol) were dissolved in ethanol (5 mL), and then sealed and subjected to an inert gas purge for 10 min. The polymer was synthesized by adding an AIBN initiator (4.1 mg, 25 μmol) followed by heating to 60 °C for 12 h. The polymer was added to diethyl ether to obtain a powder. Poly[(2-methacryloyloxyethyl phosphorylcholine)-*co*-(*n*-butyl methacrylate)]: ^{1}H NMR ($CDCl_3$/CD_3OD, 400 MHz): δ 0.83−0.94 (br, 3H), 1.39 (br, 2H), 1.59 (br, 2H), 3.22 (br, 9H), 3.65 (br, 2H), 3.91 (br, 2H), 4.00 (br, 2H), 4.13 (br, 2H), 4.23 (br, 2H).

2.3. MF of PDMS Microparticles. Uniform silicone microparticles were prepared by microfluidics by implementing slight modifications to the process used in previous studies.[16,17] An aqueous solution of 3 wt % PVA was prepared by dissolving PVA (15 g) in DI (485 mL) at 70 °C 2 h as a continuous phase. It was then vacuum-filtered to remove undissolved gel-like particles. As a dispersed phase, a 5 wt % solution of the silicone elastomer precursor (Sylgard 184, a 10:1 mixture of subject and cross-linker) was prepared by dissolving it (2.5 g) in dichloromethane (47.5 g). For the microfluidic system, the end of a syringe needle (30 G) was first inserted into a small glass capillary (outer diameter, 0.95 mm) and then connected to the inner part of a silicone tube (internal diameter, 0.79 mm).

Two syringe pumps were used to deliver a constant flow of the organic solvent phase to the needle at 0.05 mL/min and the aqueous solution phase to the glass capillary at 1.00 mL/min. Herein, the injection rate ratio of the two phases (V_c/V_d

https://doi.org/10.1021/acsomega.4c06043
ACS Omega 2024, 9, 43817−43825

≈ 20) could be adjusted to control the drop-shaped organic solvent dispersion phase size (400 μm) and the frequency of production. Conversely, a flexible silicone tube was connected to a 500 mL receiving flask to obtain a mixture of droplets of the organic solvent phase dispersed in the aqueous solution phase.

The obtained mixture was placed in a bath at 40 °C for 2 d to evaporate the organic solvent from the droplets so that the silicone precursor could be cross-linked and solidified to a proper size. Before the end of curing, a solution of zwitterionic polymer (200 μL, 100 mg/mL) was added to the mixture to allow surface modification, which was previously prepared in the same way as in our previous study, and then postcured at 60 °C for 6 h. Finally, the aqueous solution (i.e., the continuous phase) was decanted, washed 3 times with DI, and dried.[15]

2.4. Preparation of Carrier Hydrogels and Bulking Agents. Sodium hyaluronate (100 mg) was added to water (750 μL) and pH was adjusted to 13 by adding 1 M NaOH aqueous solution (250 μL). BDDE (15 μL) was then added to the mixture, and the mixture was subsequently heated at 50 °C for 3 h to yield a cross-linked hydrogel. The hydrogel was transferred to a dialysis membrane and dialyzed in PBS for 5 d. To formulate the bulking agent for tissue augmentation, the previously fabricated microparticles and the carrier hydrogel were mixed in a 2:3 weight ratio and then placed into a 1 mL syringe, which was readily available for use [i.e., zwitterion-coated PDMS HA solution by MF (ZcPH-MF), and uncoated PDMS HA solution by MF (UcPH-MF)].

2.5. Injectability of Microfluidically Fabricated Silicone Particles. To determine the injectability of microfluidically fabricated silicone particles, the plunger of a syringe was removed, and the prepared bulking agent (400 μL of ZcPH-MF or UcPH-MF) was used to fill the syringe followed by the reconnection of the plunger. With a 20 G needle fitted to the syringe tip, the syringe faced upward and was pumped to remove air. A long 50 mL vial equipped with a perforated septum in its opening was then placed, and the syringe was inserted into the hole of the septum, ensuring that the syringe flange was in good contact with the septum. A 2 mL vial was placed underneath the needle, and the plunger was compressed using a force tester. The compression force applied to the plunger was measured as the plunger was displaced by 10 mm (Figure 2).

2.6. Experiment in Protein Adsorption Using FITC-BSA. A fluorescent protein solution (0.45 g/dL) was prepared by adding PBS (3 mL) and FITC-BSA (13.5 mg) to a 10 mL glass vial. Lyophilized, microfluidically fabricated silicon particles (50 mg each for UcPH-MF and ZcPH-MF) were added to a 2 mL vial and the fluorescent protein solution (1 mL, 0.45 g/dL) was subsequently placed in the vial. The vials were then incubated at 37 °C for 2 h. They were then washed thrice with PBS by vertexing them 3 times (3 × 1 mL). Microparticles suspended in water (100 μL) were harvested using a micropipette and transferred to 96-well cell culture plates. The optical images were captured using a fluorescence microscope.

2.7. Evaluation of Cytotoxicity Using a Water-Soluble Formazan Dye. To perform experiments using a cell line, NIH/3T3 cells were subcultured for several passages. As a direct contact test, cell suspension with a density of 10^5/mL (400 μL) was then seeded in a 48-well plate and incubated in a CO_2 incubator at 37 °C for 18 h to ensure monolayered cell subconfluency. After the removal of the culture media, the bulking agents (4 μL each for ZcPH-MF or UcPH-MF) were carefully placed at the center of the cell layer. After fresh culture media (0.8 mL) were added, the cells were incubated with the bulking agents for another 24 h. Subsequently, the culture media were changed to the CCK-8 solution and incubated at 37 °C for 2 h. Colorimetric measurements of the optical density at 450 nm (OD_{450}) were performed. To determine the concentration dependence of the cell cytotoxicity, a test on material extracts was performed. The bulking agent was incubated at a concentration of 80 mg/mL in complete culture media to obtain the leachables as the original extract. Then the cytotoxicity tests were carried out down to 32-fold dilutions (2.5 mg/mL) by serially diluting the extracts.

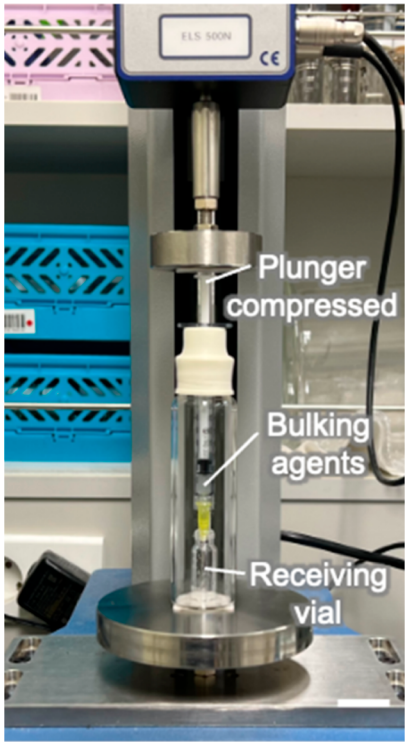

Figure 2. Experimental setup to quantify the injectability of bulking agents. A commercially available force tester was used to record the forces applied to the top of the syringe plunger.

2.8. In Vivo Experiments in the Biocompatibility of the Injectable Bulking Agent. *2.8.1. Animal Study Design.* Thirty 11 week-old female Sprague Dawley rats were used for experiments. After a week of monitoring, the rats were randomly divided into two groups (15 rats in each group). Weight deviations among the groups ranged from 242 to 278 g. The rats were intramuscularly injected with the painkiller ketoprofen (5 mg/kg) and subcutaneously injected with the antibiotic amikacin (10 mg/kg). A 3 mm Bovie incision was made on the left side of the anus (Figure 3a). The injection procedure was performed 2 weeks after the sphincter's injury. Fifteen rats were injected with ZcPH-MFs (0.1 mL) and 15 with UcPH-MFs (0.1 mL). Materials were injected into the left side of the anus at depths in the range of 6−8 mm, parallel to the rectum using a 1 mL syringe and a 20 G needle (Figure 3b). The rats were examined twice per week by a researcher (L. S.). Signs of local or systemic infections were observed and recorded.

https://doi.org/10.1021/acsomega.4c06043
ACS Omega 2024, 9, 43817−43825

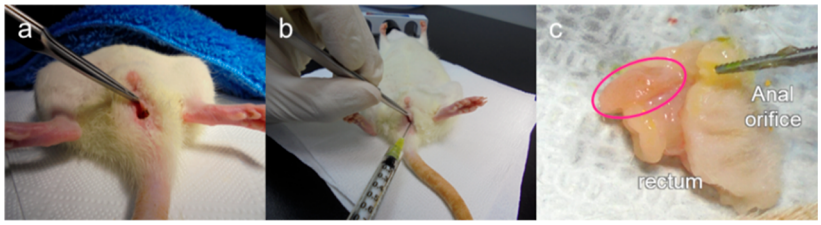

Figure 3. Bulking materials were injected into the injured anal sphincter and were removed along with surrounding tissue after 6 months. (a) A 3 mm Bovie incision was made on the left side of the anus. (b) A volume of 0.1 mL of each bulking material was injected into the anus 1 week after the sphincter's injury. (c) The bulking implant (red circle) with surrounding tissue was removed en bloc.

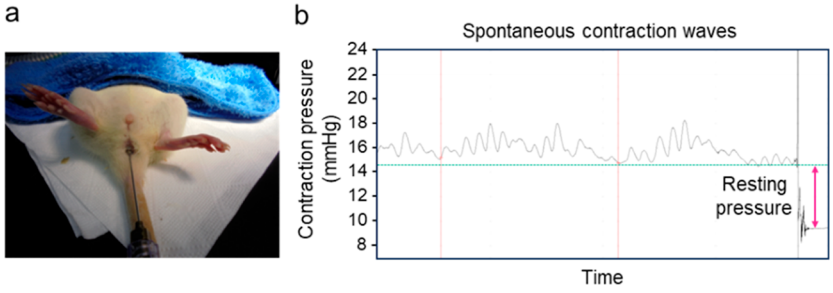

Figure 4. Balloon probe placement into the anal canal. Spontaneous contraction waves were recorded for 5−10 min. To determine the resting pressure, the balloon probe was drawn out in a contraction interval, and the resulting difference from the baseline pressure (the mean of three intervals) was calculated.

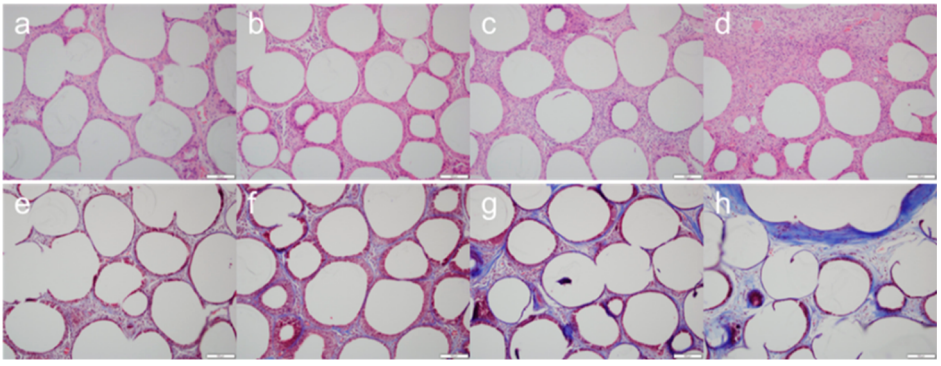

Figure 5. Microscopic evaluation of anorectal tissue around the bulking implant. H&E staining was used to obtain inflammatory scores to assess the severity of the inflammation (a−d, score 1−4). Masson's trichome staining indicate the fibrosis score on the thickness of the fibrotic band (e−h, score 1−4). Scale bar, 100 μm.

All experimental procedures were approved by the Animal Ethics Committee of the Korea University College of Medicine (IRB no. KOREA-2022-0056). All rats were sacrificed 6 months after injection. The rats were anesthetized using inhaled isoflurane and euthanized with concentrated CO_2 gas in a designated euthanasia chamber. The anorectal tissue was removed en bloc to protect the injected material (Figure 3c), and the lungs, liver, kidneys, and iliac lymph nodes were excised. The manometric evaluation was performed at baseline, after sphincter injury, and 4 and 6 months after injection.

2.8.2. Anal Manometric Evaluation. A saline-filled latex balloon (Hugo Sachs Elektronik, Germany) was used; this was connected using a stainless steel gavage feeding needle to a pressure transducer (BP-100, iWorx Systems; Dover, NH, USA), and a physiological data acquisition system (IX-TA-220 with Lab-Scribe Software, iWorx Systems; Dover, NH, USA) was employed for anal manometric measurements. The balloon size was 4 mm at baseline and after sphincter injury. The balloon size increased to 6 at 4 and 6 months after injection because the average weight of the rats increased by approximately 50% compared with that at baseline. A balloon probe inflated to pressures in the range of 12−15 mmHg was inserted into the anal canal up to 6−10 mm beyond the opening of the anus. After a 5−10 min adaptation period, spontaneous contraction waves were recorded for 5−10 min. To determine the resting pressure, the balloon probe was drawn out in a contraction interval, and the resulting difference from the baseline pressure (mean of five intervals) was calculated (Figure 4).[9]

2.8.3. Microscopic Evaluation. Paraffin-embedded sections were stained with hematoxylin and eosin (H&E). A detailed explanation of the histological process was described in a previous publication.[9] For anorectal tissue, Masson's trichome staining was performed to assess the extent of fibrosis around the bulking implants. The implant size was measured on the slide based on the length of the longest axis.

Microscopic evaluation was performed in a blinded manner by a pathologist (J.-W. Choi). When evaluating the local immune response, the number of cells per high-power field (400×) around the implant was counted, and inflammatory

https://doi.org/10.1021/acsomega.4c06043
ACS Omega 2024, 9, 43817−43825

and fibrosis scores were assigned. Each score was measured as the average of three different areas, and the highest score was estimated to be in the low-power field (100×). The inflammatory score was divided into five stages from 0 to 4 depending on the severity of the inflammation.[18] The fibrosis score was also divided into five stages (from 0 to 4) depending on the thickness of the fibrotic band (Figure 5).[9] The systemic migration of injected materials was assessed by identifying whether there were any foreign materials or an inflammatory reaction in distant organs.

2.9. Statistical Methods. The mean difference in manometric pressure at different time points in the same group was evaluated using a paired-sample *t*-test. Paired data between two groups were evaluated using an independent two-sample *t*-test. Quantitative values were summarized as means and standard errors. Values of $p \leq 0.05$ were considered statistically significant. Data analyses were performed using the software SPSS (version 20.0, IBM SPSS Statistics, Armonk, NY, USA).

3. RESULTS

3.1. Synthesis of Zwitterionic Polymers. The compositions of zwitterionic polymers play important roles in both biocompatibility and surface treatment. A greater zwitterionic composition may improve biocompatibility, albeit with a possible reduction in water stability after surface treatment. To determine zwitterion composition in the synthesized polymer, ^{1}H NMR measurements were performed. The ^{1}H NMR data showed the zwitterion composition of 0.45 (Supporting Information Figure S1). While this was a slight deviation from the targeted composition of 0.5, it was acceptable as it was in between the targeted composition and the composition of 0.3, which is established as having excellent stability in aqueous media.

3.2. Microfluidic Fabrication of Silicone Particles. The size distribution showed that the microparticles fabricated using the conventional suspension-based method had the particle diameters of 218.8 ± 73.1 and 218.0 ± 80.3 μm for UcPH and ZcPH, respectively (Figure 6). Conversely, microfluidically fabricated particles yielded the diameters of 200.4 ± 10.0 and 198.0 ± 7.3 μm for UcPH-MF and ZcPH-MF, respectively.

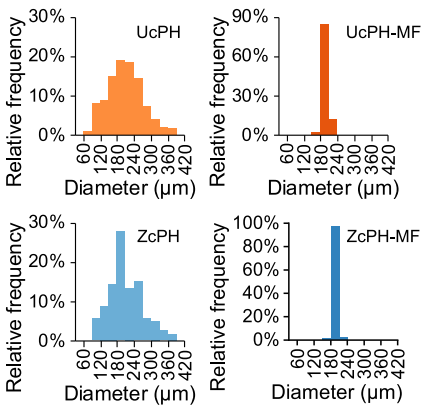

Figure 6. Percentage histograms describe the distributions of microparticles fabricated using the conventional [uncoated PDMS HA (UcPH) and zwitterion-coated PDMS HA solution (ZcPH)] and MF methods (UcPH-MF and ZcPH-MF).

In terms of the mean diameter, the particles fabricated by MF were only 1.1 times smaller than those produced by the conventional suspension-based method. In contrast, the coefficient of variance ($CV = \frac{SD}{mean}$), a standardized measure of dispersion, was smaller by as much as 10 times (36.8% [ZcPH] vs 3.7% [ZcPH-MF]).

3.3. Quantitative Measure of Injectability Using a Force Tester. The recorded injection forces were classified into baseline force (i.e., the force that was continuously applied in a given situation) and maximum force (i.e., the increased force owing to needle clogging). The calculation for baseline force was performed using the end point-weighted method by calculating the arithmetic mean of the load values.

The results yielded a maximum force in the range of 0.44−0.48 N for UcPH-MF and ZcPH-MF for microparticles that were prepared using MF, thus suggesting there was no interval which required high-injection force (Figure 7). Conversely,

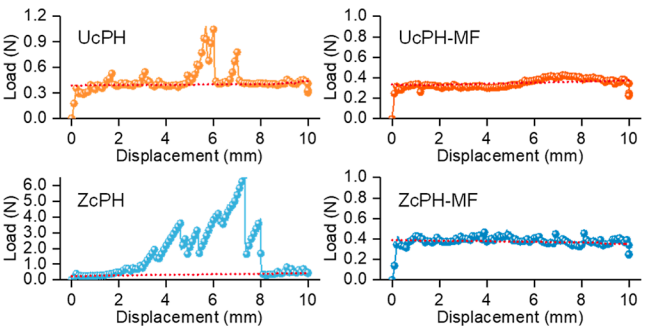

Figure 7. Injectability of bulking agents formulated with microparticles prepared using the conventional (UcPH and ZcPH) and MF methods (UcPH-MF and ZcPH-MF), and quantified based on compression forces obtained by the motorized force tester. The lines with symbols represent the applied loads during injections, while the solid straight lines represent the baseline forces calculated to yield the injection forces without any disturbances.

UcPH and ZcPH prepared using the conventional suspension-based method yielded a maximum force in the range of 1.08−6.67 N, representing a 15.2-fold increase in injection forces. Comparatively, the baseline force yielded outcomes in the ranges of 0.35−0.37 N for UcPH-MF and ZcPH-MF, and 0.34−0.40 N for UcPH and ZcPH, which were not noticeably different.

3.4. Experiments in Protein Adsorption. Protein adsorption is the first step in the FBR. It triggers a cascade of events, including cell recognition and adhesion, signal transduction, and inflammatory cellular responses. Therefore, it is a critical step that needs to be avoided in the successful implantation of biomaterials. The silicone particles focused on in this study had a highly hydrophobic surface, which resulted in a high-surface energy at the interface with water in aqueous environments, that is, in the body. This made them thermodynamically favorable for hydrophobic interactions and protein adsorption. This effect could be inhibited by modification with extremely hydrophilic zwitterionic polymers. Because silicone and zwitterionic materials are incompatible in terms of polarity, the incorporation of *n*-butyl groups as anchoring groups—that can mediate hydrophobic interactions—was employed to modify the zwitterionic polymer.[19]

The results yielded a fluorescence intensity of 7.7 for UcPH-MF with more intense fouling with the fluorescent protein

https://doi.org/10.1021/acsomega.4c06043
ACS Omega 2024, 9, 43817−43825

compared with a fluorescence intensity of only 2.11 for ZcPH-MF and revealed a 72.6% reduction in protein adsorption in the presence of zwitterions (Figure 8).

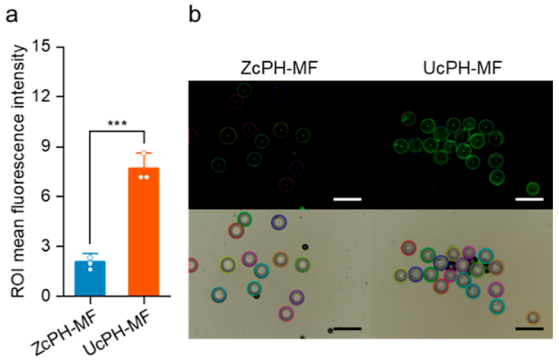

Figure 8. Protein adsorption properties characterized using the fluorescent protein, FITC-BSA. (a) Comparison of mean fluorescence intensities on the particle surfaces after protein adsorption [mean ± standard deviation (SD); Tukey's test; ***$p < 0.001$; $n = 3$]. (b) Optical and fluorescence micrographs of protein adsorbed particles based on region-of-interest measurements. Scale bar, 500 μm.

3.5. Cytotoxicity of the Bulking Agents. The concentration-dependent cytotoxicity of the bulking agents was investigated with the material extracts (Figure 9a). At the maximum concentration of the original extract, cell viability was significantly reduced to 75.5% for ZcPH-MF and 82.3% for UcPH-MF compared to control. In both samples, cross-linked HA was used as the carrier gel, which may potentially indicate chemical-induced toxicity from the cross-linker. On the other hand, there was no statistical difference between the two treatments of ZcPH-MF and UcPH-MF. The experiment in cytotoxicity using a direct contact test results yielded cell viability and proliferation outcomes of 99.4% and 94.3% for ZcPH-MF and UcPH-MF, respectively, compared with those of the control of the pristine culture (Figure 9b). In this condition (comparable to the concentration of 5 mg/mL), neither ZcPH-MFs nor UcPH-MFs had significant effects on cell viability and proliferation compared with the control (one-way analysis of variance; $F = 0.786$, $p = 0.498$) and cause any morphological change in the cells in direct contact.

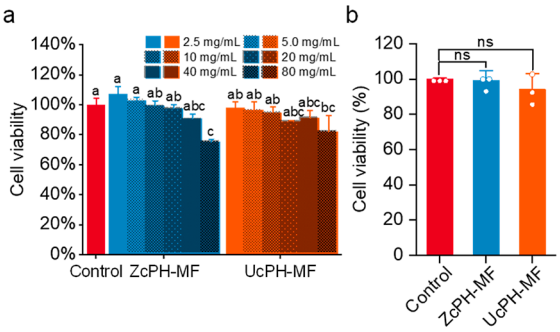

Figure 9. Cytotoxicity of the injectable bulking materials. (a) Cell viability 24 h after the treatment of material extracts and (b) cell viability 24 h after direct contact. A cell culture without any foreign material was set as the control and the cell numbers relative to the control are presented as the percent cell viability. The means that do not share a letter are statistically different ($n = 3$; mean ± SD; Tukey's test [$\alpha = 0.001$]; ns, no significance).

Nevertheless, the minor differences in the mean values and SDs could be attributed to the chemicals of PDMS and HA in the constituent materials. Unlike previous studies, the silicone precursor was not used as it was; instead, it was dissolved in the organic solvent phase for MF, which may have caused the leaching of toxic substances from the materials.[20]

3.6. Animal Experiments. One rat in the UcPH-MF group died 5 months after the bulking injection; there were no specific causes. No specific findings were observed during the gross autopsy of the organs or following the histologic examination of the perirectal tissue. The rats did not exhibit any abnormal behaviors or signs of infection during the experimental period.

3.7. Animal Manometric Evaluation. The resting pressure after sphincter injury was lower compared with the baseline, with no significant difference between the two groups (ZcPH-MF, 3.49 ± 1.37 mmHg vs UcPH-MF, 3.51 ± 1.77 mmHg, $p = 0.973$). The resting pressure 4 months and 6 months after injection respectively showed no differences between the two groups (ZcPH-MF, 3.87 ± 1.66 vs UcPH-MF, 3.79 ± 1.54, $p = 0.883$, 4 months after injection; ZcPH-MF, 3.13 ± 0.63 vs UcPH-MF, 3.10 ± 0.41, $p = 0.894$, 6 months after injection). The resting pressure 4 months and 6 months after injection treatment in each group also showed no differences (4 months after injection, 3.87 ± 1.66 vs 6 months after injection, 3.13 ± 0.63, $p = 0.092$, ZcPH-MF; 4 months after injection, 3.96 ± 1.45 vs 6 months after injection, 3.10 ± 0.41, $p = 0.082$, UcPH-MF). Overall, this analysis revealed that anal resting pressure at different time points after injection did not differ between the two groups. In each group, the resting pressure tended to decrease over time after injection.

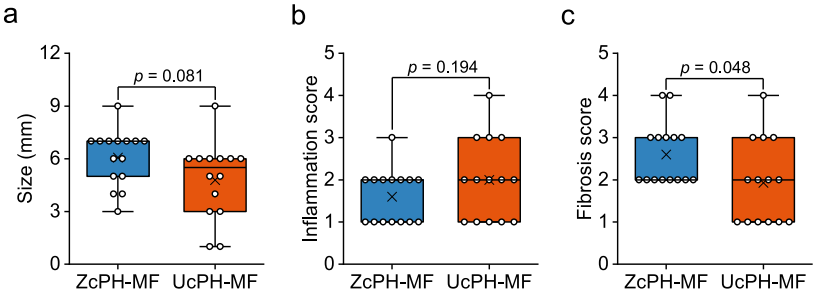

Figure 10. Three histologic indicators of the local immune reaction. (a) The size of ZcPH-MF was better preserved than that of UcPH-MF with borderline significance. (b) ZcPH-MF has a lower inflammatory score than that of UcPH-MF, but there is no statistical difference between the two results. (c) ZcPH-MF has a higher fibrosis score than that of UcPH-MF (difference is statistically significant). Data are presented as box plots with median (lines), interquartile ranges (boxes), means (x marks), minima and maxima (whiskers), and data points (open circles).

https://doi.org/10.1021/acsomega.4c06043
ACS Omega 2024, 9, 43817−43825

3.8. Histologic Analysis of the Local Immune Reaction. H&E staining showed that both ZcPH-MFs and UcPH-MFs formed well-demarcated space-occupying lesions which consisted of refractile spheres with infiltration of various inflammatory cells, such as lymphocytes, histiocytes, and giant multinucleated cells. Encapsulation of individual particles by the host tissue, as well as the entire injected mass, was observed. Masson's trichrome staining exhibited fibroblast proliferation around the individual particles.

The sizes of ZcPH-MF were better preserved without fragmentation than those of UcPH-MF. The findings exhibited borderline significance (ZcPH-MF, 6.07 ± 1.58 vs UcPH-MF, 4.79 ± 2.19, $p = 0.081$). ZcPH-MF had a lower inflammatory score than UcPH-MF, but the difference was not statistically significant (ZcPH-MF, 1.60 ± 0.63 vs UcPH-MF, 2.00 ± 0.96, $p = 0.194$). ZcPH-MF had the higher fibrosis score than that of UcPH-MF with statistical significance (ZcPH-MF, 2.60 ± 0.74 vs UcPH-MF, 1.93 ± 0.99, $p = 0.048$; Figure 10).

3.9. Evaluation of Distant Organs. No foreign material was detected histologically in the distant organs, including the lungs, liver, kidneys, or iliac lymph nodes. There was also no abnormal inflammatory reaction, such as an allergic or FBR, enabled by the possible migration of the injected materials.

4. DISCUSSION

The size distribution of microparticle biomaterials is an essential factor in medical applications. Phagocytosis can occur for particles below a certain size (e.g., 65 μm), and the inflow of phagocytic monocytes, macrophages, and neutrophils can be followed by inflammation and tissue necrosis within 4 weeks.[21,22] Among polymeric microparticulate biomaterials [e.g., polystyrene, poly(methyl methacrylate), or polytetrafluoroethylene], the phagocytosis limit for silicone particles is known to be more ambiguous owing to the properties resulting from their unique flexible chemical structure.[23] Thus, for the successful mid- to long-term implantation of silicone microparticles as a bulking agent, it is essential to follow a strict design rule with respect to their sizes. Microfluidic techniques outperform other microparticle fabrication methods (e.g., emulsion evaporation or spray drying) in terms of size controllability and uniformity, and they are also cost-effective and easy to customize.[24] To pursue the goal of examining the 6 month midterm outcomes of bulking agents, we made use of these advantages to fabricate microparticles using a simple capillary-based microfluidic device. The results highlighted the superior size tunability and uniformity of MF. Based on previous reports on other polymeric microparticles, a CV of <5% is indicative of a typical MF dispersion and suggests the successful implementation of the microfluidic technique for silicone particles in this study.

Although good injectability is beneficial for accurate and successful surgical procedures, it has been overlooked because it tends to be considered manageable with good operating dexterity. Therefore, the investigation of injectability has been largely limited to testing whether it is injectable. In this study, a reliable method for quantifying injectability was proposed to provide an objective assessment of injectability. As shown by the results, a substantial drop in maximum force was observed. This can be attributed to the elimination of needle clogging owing to the removal of particles at the large extremity of the size distribution owing to MF. For the 20 G needle, the inner diameter was 603 μm. The maximum force considerably deviated from the baseline force even though no particle size exceeded 400 μm (in the UcPH-MF and ZcPH-MF cases); accordingly, it can be inferred that particles with sizes smaller than the syringe inner diameter can also cause clogging, depending on the geometry of the particles packed near the outlet. It should also be noted that the baseline forces did not differ significantly in the microfluidically and conventionally fabricated particle cases; this can be explained by the similarity in their average sizes. Smaller variations in the injection force can induce a lower-intensity wobble at the injection sites. This can be advantageous for precise needle positioning and injection speed when injecting tissue-bulking agents into small organs, particularly in small animals where access is difficult. As significantly improved injectability was confirmed, we performed bench-stage experiments to determine biocompatibility before implantation in vivo.

In the experiment in protein adsorption, the protein inhibition effect of the zwitterions was effective and consistent, considering that the conventional suspension-based particles in our previous study were reduced by 58.5%. Zwitterionic polymers are well-known for their superhydrophilic properties, which enable them to form a thick hydration layer on their surfaces. This hydration layer effectively blocks protein adsorption by creating a barrier that proteins cannot easily penetrate. The strong interaction between water molecules and the zwitterionic groups is key to the mechanism. As a result, zwitterionic polymers are highly effective in preventing biofouling. In addition, although the codispersant used for stabilizing the droplets was changed from polyvinylpyrrolidone to PVA during the preparation of the particles, the effectiveness of the zwitterion was maintained. Because the silicone material surface has structural flexibility at the molecular level, it easily loses its introduced hydrophilicity owing to molecular rearrangement in air. However, the aqueous environment of the enclosing carrier gel effectively suppressed this tendency. Before a biomaterial can be safely and effectively used in the body, it should be rigorously evaluated for biocompatibility. One of the key material aspects of biocompatibility is cytotoxicity, which refers to the potential of a substance to damage or kill living cells. Cytotoxicity testing can reveal adverse effects of biomaterials at the cellular and tissue levels and help optimize their design and formulation. Cytotoxicity testing in the present study was performed by directly exposing cells to biomaterials. We hypothesized that our newly fabricated bulking agent had low cytotoxicity and high biocompatibility because it was composed of HA and silicone, which are considered the most biocompatible materials. The results showed no significant cell cytotoxicity in the cases of the bulking agents used in conjunction with MF; these findings justified the sequential preclinical testing in vivo. No signs of foreign materials or inflammation were observed in distant organs. Most PDMS particles in the filler exceeded 100 μm in diameter; hence systematic migration was expected to be inherently unlikely. However, this needs to be confirmed through repeated experiments at different injection sites.

The MF provided good injectability without resistance at the tissue level with a 20 G needle. We needed to use an 18 G needle in a previous study to inject bulking material manufactured with the same substances without the use of MF.[9] Smaller needle diameters enabled us to inject substances more precisely into perianal muscles. This advantage is expected to cause less pain to patients and enable more accurate injections in clinical practice.

https://doi.org/10.1021/acsomega.4c06043
ACS Omega 2024, 9, 43817−43825

In the manometric experiments, we did not observe any differences in the resting pressure between the two bulking materials. This lack of differences could be because the resting pressure values yielded mixed results, even in clinical practice.[1] The variability in physiological responses may stem from the lack of clear elucidation regarding the mechanisms governing the function of bulking agents. In human studies, the interpretation of results often relies on diverse indicators including rectal sensation, maximal tolerable volume, and anal resting pressure measured using anal manometry, all of which involve direct communication with patients. In addition, the limited thickness of the anal sphincter complex in rats (<2 mm) may affect the precision of the pressure measurements in the anal canal. While some studies utilizing FI rat models have demonstrated the feasibility of the approach, larger animal models with more injections may be better suited for investigating the specific function of the anal sphincter.[25,26]

Histological analysis indicated that the preservation of ZcPH-MF size was superior to that of UcPH-MF size, albeit with borderline significance. This aligns with the findings of the in vitro test that showed a 72.7% reduction in protein adsorption in the presence of zwitterions. Reduced protein adsorption likely contributes to the increased durability of the bulking implant by circumventing the immune response and inhibiting phagocytosis. Unlike prior studies with short-term followups, the observed difference in durability could be attributed to the longer 6 month followup in this animal experiments.[9]

The inflammatory score reflects an early FBR, which usually reaches a peak 1−4 weeks after implantation.[3] The initial inflammatory reaction is then followed by a fibrosis process repairing the damaged tissue. The nature of these reactions depends on the host immune system. Our experimental followup period of 6 months may thus be insufficient for investigating inflammatory reactions. However, compared with a previous study (wherein the followup period was 4 weeks), the inflammatory score decreased over time, and ZcPH-MF had a lower inflammatory score than UcPH-MF, even at different time points, although the difference was not statistically significant. This suggests that a reduction in protein adsorption in the presence of zwitterions can reduce the inflammatory process in FBRs.

Initially, we hypothesized that reduced protein adsorption onto bulking implants derived from the surface coating of hydrophilic zwitterions would reduce FBRs. Fibrosis is caused by tissue remodeling and the late phase of an FBR. However, interestingly, ZcPH-MFs had a significantly higher fibrosis score than UcPH-MFs. Compared with a previous study with a short-term followup period of 4 weeks, ZcPH-MF resulted in a higher fibrosis score over time. Regarding this result, we can speculate that hydrophilic particles coated with zwitterions are less readily phagocytosed.[27] The failure of effective phagocytosis can lead to granuloma formation and encapsulation. Many macrophages that are unable to digest foreign bodies can aggregate into multinuclear giant cells (diameters ranging from 40 to 50 μm). To develop more stable granulomas, there is a surrounding rim of fibroblasts and connective tissue encapsulating the foreign body.[28] This effective encapsulation process has the potential to induce immune evasion, thereby halting sustained inflammatory responses on the implant surface. Furthermore, particle encapsulation serves as a framework for securely anchoring microparticles to adjacent host tissues, thereby mitigating migration-related complications.

No signs of foreign material or inflammation were observed in distant organs. Given that the uniformly sized particles (manufactured by MF) are larger than the in vivo migratory limit of 80 μm, systematic migration was anticipated to be inherently improbable.

Future studies should consider the use of larger animal models. Because rats have small rectal and anal muscles, access and maneuvering within their anorectal regions can be challenging. Consequently, assessing how these small muscles control bowel movements using manometry—which is typically intended for use in larger animals, such as humans—is more difficult for small animals. Finally, long-term results should be monitored to compare the materials' performances.

5. CONCLUSIONS

In conclusion, this study highlights the significance of silicone fillers with uniform microsized diameters and surface treatment in medical applications, particularly in the context of bulking agents. MF offers advantages in size tunability and uniformity compared with conventional methods, thereby improving injectability and potentially reducing the risk of complications, such as treatment failure. Not only did the protein adsorption experiment yield promising results with zwitterion-coated fillers, suggesting improved biocompatibility and durability, but the cytotoxicity experiment confirmed the safety of these fillers in vitro. In vivo animal studies have demonstrated improved injectability and potential advantages in tissue response. Nevertheless, further investigation is needed, particularly with regard to long-term outcomes and the use of larger animal models.

■ ASSOCIATED CONTENT

Supporting Information

The Supporting Information is available free of charge at https://pubs.acs.org/doi/10.1021/acsomega.4c06043.

^{1}H NMR spectra for all compounds (PDF)

■ AUTHOR INFORMATION

Corresponding Authors

Ji-Hun Seo − *Department of Materials Science and Engineering, Korea University, Seoul 02841, Republic of Korea*; orcid.org/0000-0001-6193-4008; Email: seojh79@korea.ac.kr

Kwang Dae Hong − *Department of Colorectal Surgery, Korea University Ansan Hospital, Ansan-si, Gyeonggi-do 15355, Republic of Korea*; Email: drhkd@korea.ac.kr

Authors

Joonbum Lee − *Department of Materials Science and Engineering, Korea University, Seoul 02841, Republic of Korea*

Jung-Woo Choi − *Department of Pathology, Korea University Ansan Hospital, Ansan-si, Gyeonggi-do 15355, Republic of Korea*

Sang-A Lee − *Department of Colorectal Surgery, Korea University Ansan Hospital, Ansan-si, Gyeonggi-do 15355, Republic of Korea*

https://doi.org/10.1021/acsomega.4c06043
ACS Omega 2024, 9, 43817−43825

Seokhyun Jang − *Department of Materials Science and Engineering, Korea University, Seoul 02841, Republic of Korea*

Complete contact information is available at: https://pubs.acs.org/10.1021/acsomega.4c06043

Author Contributions

‖J.L. and J.-W.C. contributed equally. The manuscript was written through contributions of all authors. All authors have given approval to the final version of the manuscript. **Joonbum Lee**: Investigation, Visualization, Writing−original draft. **Jung-Woo Choi**: Investigation, Data curation, Writing−original draft. **Sang-A Lee**: Resources, Investigation. **Seokhyun Jang**: Resources, Investigation. **Ji-Hun Seo**: Supervision, Conceptualization, Writing−review and editing. **Kwang Dae Hong**: Supervision, Methodology, Writing−review and editing.

Notes

The authors declare no competing financial interest.

■ ACKNOWLEDGMENTS

This research was supported by the National Research Foundation of Korea Grant funded by the Korean Government [NRF-2022R1A2C2009877] and the Yangyoung Research Foundation of Korea.

■ REFERENCES

(1) Hong, K. D.; Kim, J. S.; Ji, W. B.; Um, J. W. Midterm outcomes of injectable bulking agents for fecal incontinence: a systematic review and meta-analysis. *Tech. Coloproctol.* **2017**, *21* (3), 203−210.

(2) Graf, W.; Mellgren, A.; Matzel, K. E.; Hull, T.; Johansson, C.; Bernstein, M. Efficacy of dextranomer in stabilised hyaluronic acid for treatment of faecal incontinence: a randomised, sham-controlled trial. *Lancet* **2011**, *377* (9770), 997−1003.

(3) Anderson, J. M.; Rodriguez, A.; Chang, D. T. Foreign body reaction to biomaterials. *Semin. Immunol.* **2008**, *20* (2), 86−100.

(4) Harlim, A.; Kanoko, M.; Aisah, S. Classification of Foreign Body Reactions due to Industrial Silicone Injection. *Dermatol. Surg.* **2018**, *44* (9), 1174−1182.

(5) Fournier, E.; Passirani, C.; Montero-Menei, C. N.; Benoit, J. P. Biocompatibility of implantable synthetic polymeric drug carriers: focus on brain biocompatibility. *Biomaterials* **2003**, *24* (19), 3311−3331.

(6) Cao, B.; Tang, Q.; Cheng, G. Recent advances of zwitterionic carboxybetaine materials and their derivatives. *J. Biomater. Sci., Polym. Ed.* **2014**, *25* (14−15), 1502−1513.

(7) Liu, Y.; Zhang, F.; Lang, S.; Yang, L.; Gao, S.; Wu, D.; Liu, G.; Wang, Y. A Uniform and Robust Bioinspired Zwitterion Coating for Use in Blood-Contacting Catheters with Improved Anti-Inflammatory and Antithrombotic Properties. *Macromol. Biosci.* **2021**, *21* (12), No. e2100341.

(8) Diaz Blanco, C.; Ortner, A.; Dimitrov, R.; Navarro, A.; Mendoza, E.; Tzanov, T. Building an antifouling zwitterionic coating on urinary catheters using an enzymatically triggered bottom-up approach. *ACS Appl. Mater. Interfaces* **2014**, *6* (14), 11385−11393.

(9) Choi, J. W.; Lee, J.; Lee, Y.; Seo, J. H.; Hong, K. D. Preclinical testing of an anal bulking agent coated with a zwitterionic polymer in a fecal incontinence rat model. *J. Mater. Chem. B* **2022**, *10* (14), 2708−2718.

(10) Serati, M.; Braga, A.; Salvatore, S.; Torella, M.; Di Dedda, M. C.; Scancarello, C.; Cimmino, C.; De Rosa, A.; Frigerio, M.; Candiani, M.; Ruffolo, A. F. Up-to-Date Procedures in Female Stress Urinary Incontinence Surgery: A Concise Review on Bulking Agents Procedures. *Medicina* **2022**, *58* (6), 775.

(11) Li, X.; Du, L.; Lu, J.-j. A Novel Hypothesis of Visual Loss Secondary to Cosmetic Facial Filler Injection. *Ann. Plast. Surg.* **2015**, *75* (3), 258−260.

(12) Chae, S. Y.; Lee, K. C.; Jang, Y. H.; Lee, S.-J.; Kim, D. W.; Lee, W. J. A Case of the Migration of Hyaluronic Acid Filler from Nose to Forehead Occurring as Two Sequential Soft Lumps. *Ann. Dermatol.* **2016**, *28* (5), 645−647.

(13) Lee, J. S.; Cho, J. H.; An, S.; Shin, J.; Choi, S.; Jeon, E. J.; Cho, S.-W. In Situ Self-Cross-Linkable, Long-Term Stable Hyaluronic Acid Filler by Gallol Autoxidation for Tissue Augmentation and Wrinkle Correction. *Chem. Mater.* **2019**, *31* (23), 9614−9624.

(14) Wu, J.; Yadavali, S.; Lee, D.; Issadore, D. A. Scaling up the throughput of microfluidic droplet-based materials synthesis: A review of recent progress and outlook. *Appl. Phys. Rev.* **2021**, *8* (3), 031304.

(15) Lee, J.; Choi, J.-W.; Hong, K. D.; Seo, J.-H. Injectable polydimethylsiloxane microfiller coated with zwitterionic polymer for enhanced biocompatibility. *Colloids Surf., B* **2022**, *210*, 112223.

(16) Chung, E.-J.; Jun, D.-R.; Kim, D.-W.; Han, M.-J.; Kwon, T.-K.; Choi, S.-W.; Kwon, S. K. Prevention of polydimethylsiloxane microsphere migration using a mussel-inspired polydopamine coating for potential application in injection therapy. *PLoS One* **2017**, *12* (11), No. e0186877.

(17) Jun, D.-R.; Moon, S.-K.; Choi, S.-W. Uniform polydimethylsiloxane beads coated with polydopamine and their potential biomedical applications. *Colloids Surf., B* **2014**, *121*, 395−399.

(18) Duranti, F.; Salti, G.; Bovani, B.; Calandra, M.; Rosati, M. L. Injectable hyaluronic acid gel for soft tissue augmentation. A clinical and histological study. *Dermatol. Surg.* **1998**, *24* (12), 1317−1325.

(19) Seo, J.-H.; Hirata, M.; Kakinoki, S.; Yamaoka, T.; Yui, N. Dynamic polyrotaxane-coated surface for effective differentiation of mouse induced pluripotent stem cells into cardiomyocytes. *RSC Adv.* **2016**, *6* (42), 35668−35676.

(20) Meng, E.; Sheybani, R. Insight: implantable medical devices. *Lab Chip* **2014**, *14* (17), 3233−3240.

(21) Allen, O. Response to subdermal implantation of textured microimplants in humans. *Aesthetic Plast. Surg.* **1992**, *16* (3), 227−230.

(22) Tomazic-Jezic, V. J.; Merritt, K.; Umbreit, T. H. Significance of the type and the size of biomaterial particles on phagocytosis and tissue distribution. *J. Biomed. Mater. Res.* **2001**, *55* (4), 523−529.

(23) Morhenn, V. B.; Lemperle, G.; Gallo, R. L. Phagocytosis of different particulate dermal filler substances by human macrophages and skin cells. *Dermatol. Surg.* **2002**, *28* (6), 484−490.

(24) Long, F.; Guo, Y.; Zhang, Z.; Wang, J.; Ren, Y.; Cheng, Y.; Xu, G. Recent Progress of Droplet Microfluidic Emulsification Based Synthesis of Functional Microparticles. *Global Challenge* **2023**, *7* (9), 2300063.

(25) Zutshi, M.; Salcedo, L. B.; Zaszczurynski, P. J.; Hull, T. L.; Butler, R. S.; Damaser, M. S. Effects of Sphincterotomy and Pudendal Nerve Transection on the Anal Sphincter in a Rat Model. *Dis. Colon Rectum* **2009**, *52* (7), 1321−1329.

(26) Salcedo, L.; Damaser, M.; Butler, R.; Jiang, H.-H.; Hull, T.; Zutshi, M. Long-Term Effects on Pressure and Electromyography in a Rat Model of Anal Sphincter Injury. *Dis. Colon Rectum* **2010**, *53* (8), 1209−1217.

(27) Bentkover, S. H. The Biology of Facial Fillers. *Facial Plast. Surg.* **2009**, *25* (02), 073−085.

(28) Kumar, V.; Cotran, R. S.; Robbins, S. L. *Robbins Basic Pathology*; Saunders, 2003.